Benchmark map of forest carbon stocks in tropical regions across three continents

Sassan S. Saatchi[a,b,1], Nancy L. Harris[c], Sandra Brown[c], Michael Lefsky[d], Edward T. A. Mitchard[e], William Salas[f], Brian R. Zutta[a,b], Wolfgang Buermann[b], Simon L. Lewis[g], Stephen Hagen[f], Silvia Petrova[c], Lee White[h], Miles Silman[i], and Alexandra Morel[j]

[a]Jet Propulsion Laboratory, California Institute of Technology, Pasadena, CA 91109; [b]Institute of Environment, University of California, Los Angeles, CA 90095; [c]Winrock International, Ecosystem Services Unit, Arlington, VA 22202; [d]College of Natural Resources, Colorado State University, Fort Collins, CO 80523; [e]Institute of Geography, School of Geosciences, University of Edinburgh, Edinburgh EH8 9XP, United Kingdom; [f]Applied GeoSolutions, Durham, NH 03824; [g]Earth and Biosphere Institute, University of Leeds, Leeds LS2 9JT, United Kingdom; [h]Agence Nationale des Parcs Nationaux, République Gabonaise, BP 20379 Gabon; [i]Department of Biology, Wake Forest University, Winston-Salem, NC 27106; and [j]Environmental Change Institute, University of Oxford, Oxford OX1 3QY, United Kingdom

Edited* by Susan E. Trumbore, University of California, Irvine, CA, and approved May 5, 2011 (received for review December 28, 2010)

Developing countries are required to produce robust estimates of forest carbon stocks for successful implementation of climate change mitigation policies related to reducing emissions from deforestation and degradation (REDD). Here we present a "benchmark" map of biomass carbon stocks over 2.5 billion ha of forests on three continents, encompassing all tropical forests, for the early 2000s, which will be invaluable for REDD assessments at both project and national scales. We mapped the total carbon stock in live biomass (above- and belowground), using a combination of data from 4,079 in situ inventory plots and satellite light detection and ranging (Lidar) samples of forest structure to estimate carbon storage, plus optical and microwave imagery (1-km resolution) to extrapolate over the landscape. The total biomass carbon stock of forests in the study region is estimated to be 247 Gt C, with 193 Gt C stored aboveground and 54 Gt C stored belowground in roots. Forests in Latin America, sub-Saharan Africa, and Southeast Asia accounted for 49%, 25%, and 26% of the total stock, respectively. By analyzing the errors propagated through the estimation process, uncertainty at the pixel level (100 ha) ranged from ±6% to ±53%, but was constrained at the typical project (10,000 ha) and national (>1,000,000 ha) scales at *ca*. ±5% and *ca*. ±1%, respectively. The benchmark map illustrates regional patterns and provides methodologically comparable estimates of carbon stocks for 75 developing countries where previous assessments were either poor or incomplete.

forest biomass | forest height | microwave and optical imaging | error propagation | carbon cycling

Deforestation and forest degradation, located primarily in tropical regions, accounted for 12–20% of global anthropogenic greenhouse gas (GHG) emissions in the 1990s and early 2000s (1–4) and these processes also impact the future potential of forests to remove additional carbon from the atmosphere (5–7). Estimates of GHG emissions from deforestation require information on both the area of forest loss and the corresponding carbon stock of the land that is cleared (8, 9). Both are considered challenging to quantify accurately (10). Much of the emphasis to date has focused on improving spatially represented estimates of forest area loss (11, 12). To improve confidence in estimated emissions, equal emphasis is needed on improving spatially explicit estimates of carbon stored in forests, which remain uncertain in tropical regions (13). The largest proportion of this uncertainty is in estimates of aboveground biomass (14, 15), which accounts for 70–90% of forest biomass carbon (16), and its spatial variability that depends on factors such as climate, human and natural disturbance and recovery, soil type, and topographical variations (14, 17). Reducing the uncertainty in emissions estimates requires temporally constrained estimates of forest carbon content at a spatial scale that is fine enough to capture the variability over the landscape and is quantified at the scale of disturbance affecting the forest. Such information would improve project- and national-level carbon stock estimates as well as assist in the development of baseline information required for reducing emissions from deforestation and degradation (REDD) activities designed to curb greenhouse gas emissions from the land use sector (15, 18).

Efforts to estimate the distribution of biomass rely on remote sensing techniques due to the wide geographical extent of forests, difficult accessibility, and the limited utility of field inventories owing to the natural spatial variability of forest biomass (8, 9, 14). New remote sensing approaches using light detection and ranging (Lidar) and radio detection and ranging (radar) from airborne sensors have been successful in providing high-resolution estimates of forest carbon density for small areas (19–21). However, the spaceborne sensors needed to use these approaches for large-scale mapping and monitoring efforts will not be available before the end of this decade (22). Until then, cost-effective mapping of carbon stocks for project- and national-scale assessments will rely on a combination of satellite imagery and ground-based inventory samples of forest carbon density (14, 21).

Here, we report on our use of global forest height data measured by the Geoscience Laser Altimeter System (GLAS), onboard the Ice, Cloud, and land Elevation Satellite (ICESat) (23), in combination with other remote sensing data bases and ground data, to model the spatial distribution of aboveground standing biomass density (AGB) (in megagrams of mass per unit area) in forests across three continental regions for the early 2000s. Our approach includes >3 million Lidar shots collected along the ICESat orbital tracks. For calibration of GLAS Lidar height to AGB and for validation of AGB distribution, we use AGB data from 4,079 available inventory and research plots distributed over the study region. We estimate belowground biomass carbon in roots from AGB using tree allometry (24). Our approach results in a benchmark map of forest carbon density at 1-km resolution. The accuracy of carbon estimates for every pixel is evaluated by propagating individual components of uncertainty through the spatial analysis.

Results

Relating Forest Height to Biomass. AGB estimates were compiled for 4,079 geo-referenced in situ forest plots (>0.1 ha) distributed over three continents and restricted to inventory dates between 1995 and 2005 (Fig. S1 and Table S1). Of these data, 493 calibration plots (298 in Latin America, 75 in Africa, and 120 in Southeast Asia) were located under the GLAS Lidar shots or within the same forest stands (Table S2). Data for these plots

ENVIRONMENTAL SCIENCES

Author contributions: S.S.S., N.L.H., S.B., and W.S. designed research; S.S.S., N.L.H., S.B., M.L., and E.T.A.M. performed research; S.S.S., N.L.H., S.H., L.W., M.S., and A.M. contributed new reagents/analytic tools; S.S.S., N.L.H., S.B., M.L., E.T.A.M., W.S., B.R.Z., W.B., S.L.L., S.P., L.W., M.S., and A.M. analyzed data; and S.S.S., N.L.H., S.B., and S.L.L. wrote the paper.

The authors declare no conflict of interest.

*This Direct Submission article had a prearranged editor.

[1]To whom correspondence should be addressed. E-mail: saatchi@jpl.nasa.gov.

This article contains supporting information online at www.pnas.org/lookup/suppl/doi:10.1073/pnas.1019576108/-/DCSupplemental.

included tree height, basal area, and AGB over an area of 0.25–1.0 ha (*SI Materials and Methods*). We used these plots to develop a power-law functional relationship (AGB = aH^k, R^2 = 0.85, $P < 0.0001$) between the ground-measured Lorey's height (basal area weighted height of all trees >10 cm in diameter) and AGB derived from allometric equations based on harvested trees (Fig. 1*A*). The relationship, including all 493 calibration plots over three continents, was tested for consistency in AGB predictions and root mean square error (RMSE) values against region-specific relationships (Fig. 1 *B*–*D*). Regional estimates outperformed the combined estimate, with the AGB predictions for a single region obtained by using a relationship developed for a different region, increasing the RMSE by 5–15%. The largest error resulted when AGB in tropical Asia was estimated from the combined continental relationship (12% increase in RMSE) or from the regional relationship developed for Latin America or Africa (15% and 13%, respectively). The combined relationship provided a consistent approach to convert Lorey's height to AGB over all forests in the study region with an overall uncertainty of ±23.8%. However, region-specific relations had higher accuracy and were used to convert a similar height metric obtained from GLAS data to AGB with an estimation uncertainty of ±15.8% in Latin America, ±21.7% in Africa, and ±25.1% in Asia. To create AGB samples at mapping units of 100 ha (1-km resolution), we aggregated five or more GLAS Lidar shots in 1-km resolution cells to produce 160,918 pixel samples that were combined with ground inventory data to model the spatial distribution of AGB (*SI Materials and Methods*).

Spatial Modeling of Forest AGB. We used a data fusion model based on the maximum entropy (MaxEnt) approach (*SI Materials and Methods*) as well as spatial imagery from multiple sensors [moderate resolution imaging spectroradiometer (MODIS), shuttle radar topography mission (SRTM), and quick scatterometer (QSCAT)] on earth-observing satellites to extrapolate AGB measurements from inventory plots and GLAS data to the entire landscape. The model produced a map of AGB along with estimates of uncertainty at a spatial resolution of 1 km (Fig. 2*A*). Forest area in each AGB range class [in millions (10^6) of hectares] and total AGB [in millions of metric tons (Mt) (1 t = 1 Mg)] were computed for each continent by using the most inclusive fractional tree cover threshold from the MODIS vegetation continuous field product (*SI Materials and Methods*) to define forests (10% tree cover). Latin America has 47% of its forest area in high biomass classes (AGB > 100 Mg ha^{-1}) (Fig. 2*B*) compared with 27% in Africa (Fig. 2*C*) and 56% in Asia (Fig. 2*D*). Nearly 75% of Africa's forests are distributed in woodland savannas and dry forests that contain low biomass (AGB < 100 Mg ha^{-1}). In Latin America, similar forests cover the cerrado of Brazil, woodlands of Argentina and Chile, and dry forests and savanna woodlands of Central and South America. In tropical Asia, low biomass density forests (44% of the area) also include secondary and degraded forests that are widespread throughout the region (24).

Although not as extensive in terms of area, forests with AGB > 100 Mg ha^{-1} contain most of the biomass on each continent, with 83%, 59%, and 82% of all biomass found in high biomass classes in Latin America (Fig. 2*E*), Africa (Fig. 2*F*), and Asia (Fig. 2*G*), respectively. Forests with AGB > 250 Mg ha^{-1} contain nearly half of all forest biomass on each continent (41% in Latin America, 38% in Africa, and 50% in Asia). Forests in the highest biomass class (AGB > 350 Mg ha^{-1}) alone comprise a significant percentage of total biomass (7.4% in Latin America, 8.7% in Africa, 7% in Asia), and they cover areas of Papua New Guinea and central Borneo (Indonesia) in Asia, western Congo Basin in Gabon and southern Cameroon, eastern Democratic Republic of Congo in Africa, eastern and northern Amazonia along the Guiana Shield, and southwestern Peru in Latin America. Similar general patterns have been observed from analysis of ground surveys (6, 25, 26). However, comparison with an earlier map of AGB over the Amazon Basin (14) revealed differences in central and western Amazonia, particularly in the Rio Negro Basin. The earlier Amazon AGB map showed higher biomass values in the central region but with large uncertainties due to a lack of ground plots (14). The forests of the Rio Negro Basin are dominated by swamp forests (*varzea*) and white sand vegetation (*caatinga* and *campinarana*) with relatively low biomass density. In western Amazonia, around the foothill of the Andes, the earlier AGB

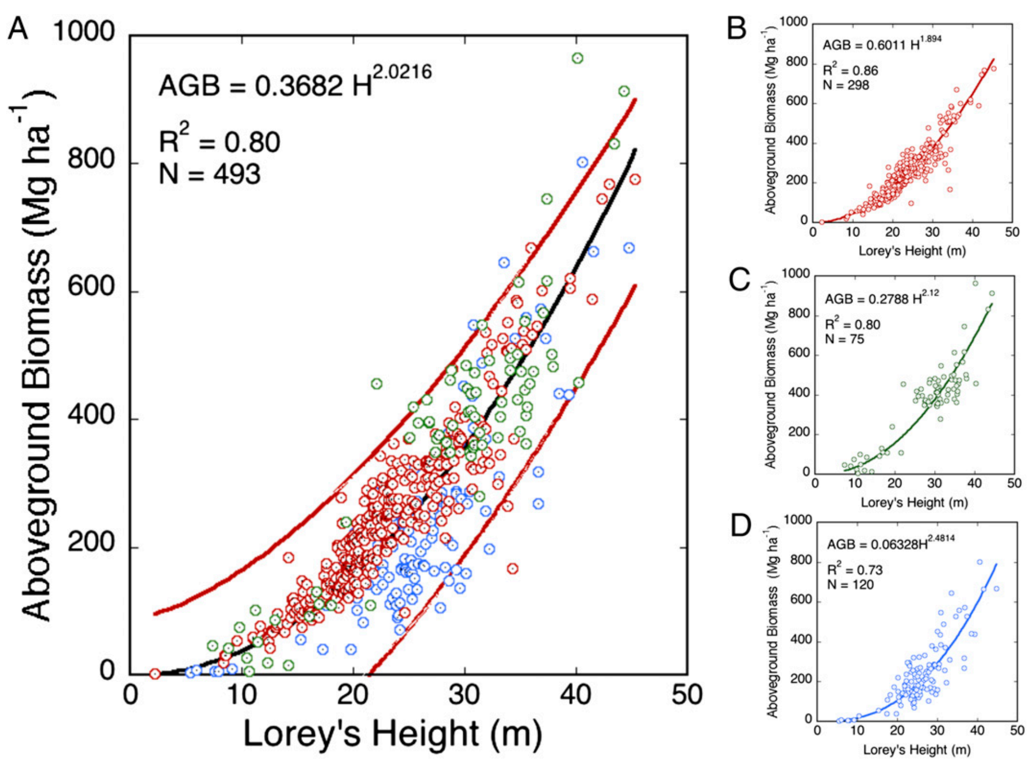

Fig. 1. Allometric relations between Lorey's height and aboveground biomass of calibration plots at spatial scales comparable to GLAS footprints. (*A*) Combined relation from three continents (AGB = $0.3104H^{2.0608}$, R^2 = 0.85, $P < 0.001$). (*B*–*D*) Allometric relation (*B*) from 298 plots in Latin America (AGB = $0.4574H^{1.9701}$, R^2 = 0.89, $P < 0.001$), (*C*) from 75 plots in sub-Saharan Africa including woodland savanna (AGB = $0.3542H^{2.0528}$, R^2 = 0.85, $P < 0.001$), and (*D*) from 120 plots in Southeast Asia including plots in secondary and fragmented forests (AGB = $0.0508H^{2.5213}$, R^2 = 0.79, $P < 0.001$).

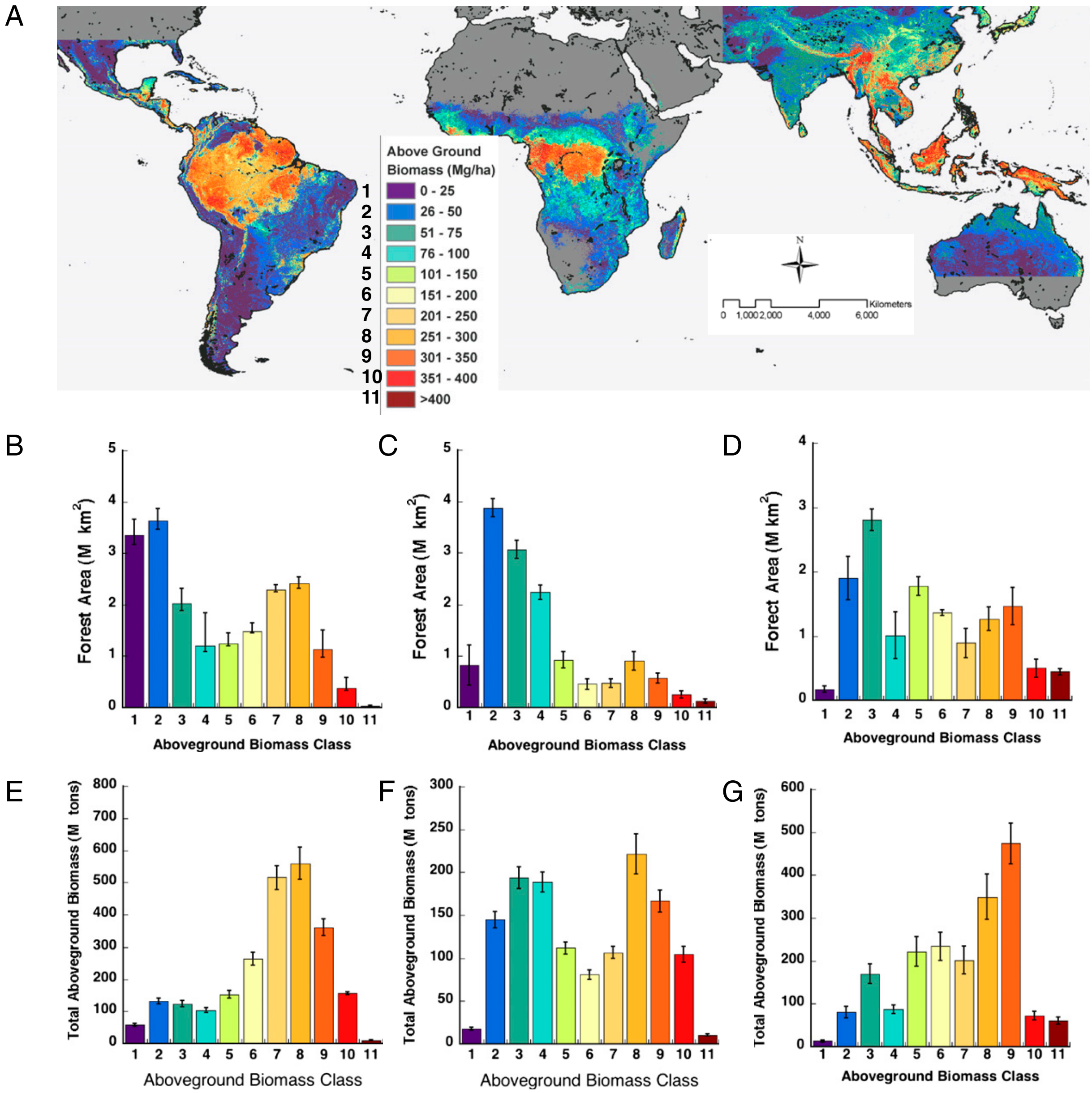

Fig. 2. Distribution of forest aboveground biomass (circa 2000). (*A*) Forest aboveground biomass is mapped at 1-km spatial resolution. The study region was bounded at 30° north latitude and 40° south latitude to cover forests of Latin America and sub-Saharan Africa and from 60° to 155° east and west longitude. The map was colored on the basis of 25–50 Mg ha^{-1} AGB classes to better show the overall spatial patterns of forest biomass in tropical regions. Histogram distributions of forest area (at 10% tree cover) for each biomass class were calculated by summing the pixels over Latin America in *B*, Africa in *C*, and Asia in *D*. Similarly, total AGB for each class was computed by summing the values in each region with distributions provided for Latin America in *E*, Africa in *F*, and Asia in *G*. All error bars were computed by using the prediction errors (*SI Materials and Methods*) from spatial modeling.

map predicted much lower biomass compared with the new benchmark map, but with higher uncertainty. These forests were mapped with less uncertainty in the new benchmark map due to the extensive GLAS Lidar sampling of forest structure.

National Assessment of Carbon Stocks. To estimate total biomass carbon stocks and produce a forest carbon "benchmark" map against which future changes can be assessed, we calculated belowground biomass (BGB) as a function of AGB (BGB = 0.489 AGB$^{0.89}$) (Fig. S2) and estimated total carbon as 50% of total biomass (AGB + BGB) (27) (Fig. 3*A*). We defined forest extent using three fractional cover thresholds (10%, 25%, and 30% tree cover) based on the range of thresholds used by individual Parties to the United Nations Framework Convention on Climate Change (UNFCCC) proceedings (28) and estimated total carbon stored in forests of each country in the study area (Table S3). In Table 1, we present the five countries per continental region that contain the highest forest carbon stocks, along with continental totals. From this analysis, we estimate the total forest biomass carbon stocks at 10% tree cover as 247 Gt C, with 193 Gt C in AGB and 54 Gt C in BGB. Forests in Latin America are the most extensive and contain ~49% of the total biomass carbon, followed by 26% in Asia and 25% in Africa. Applying a higher tree cover threshold (30%) eliminates large areas of savanna woodlands in Africa from the forest domain and reduces the total carbon stock to 208 Gt C (16% reduction with 163 Gt C for AGB and 45 Gt C for BGB). Among the countries analyzed, Brazil, the Democratic Republic of Congo, and Indonesia have the largest area of forest as well as the highest carbon stocks (62, 24, and 24 Gt C, respectively, at 10% tree cover). These esti-

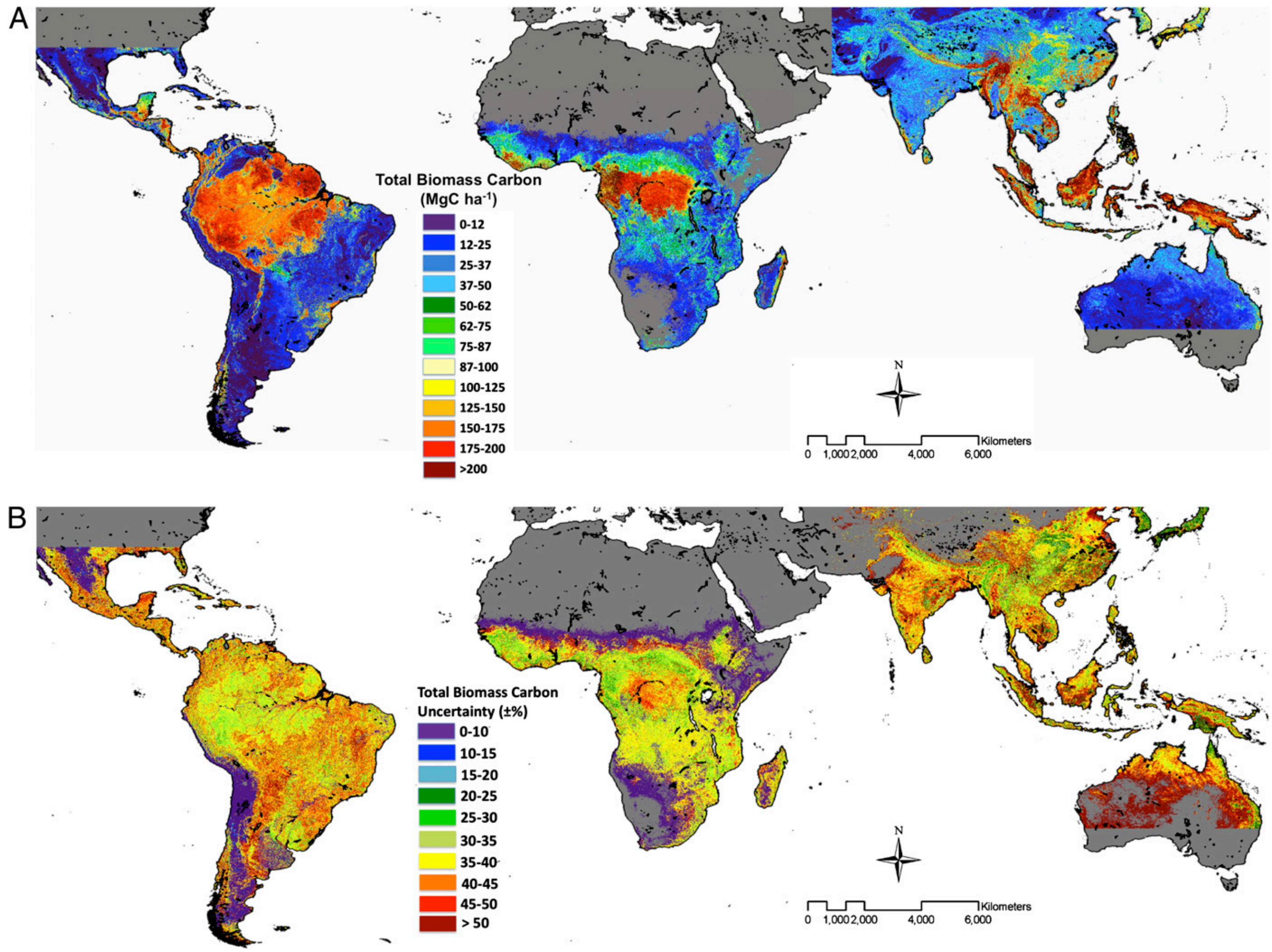

Fig. 3. Benchmark map of carbon stock and uncertainty. (*A*) Forest carbon stock defined as 50% of AGB + BGB is mapped at 1-km pixel resolution and colored on the basis of a 12–25 Mg C ha^{-1} range to show the spatial patterns. (*B*) The uncertainty of the benchmark map is estimated using error propagation through a spatial modeling approach. The uncertainty is given in terms of plus or minus percent and it includes all errors associated with prediction from spatial modeling, estimation of Lorey's height from GLAS, estimation of AGB from Lorey's height, errors from pixel level variations, and errors associated with BGB estimation (*SI Materials and Methods*).

mates improve on forest carbon stock estimates reported previously (8, 13–15, 17, 18, 25) by providing a traceable and systematic approach to geographically locate the stock estimates for further monitoring and verification. The forest definitions chosen here using tree cover thresholds can readily change the estimates of total carbon and area-weighted carbon densities at national and regional scales.

Uncertainty Analysis. We assess the accuracy of the biomass carbon estimates by calculating the error as the difference between the true mean biomass value (bootstrapped samples of ground and Lidar-estimated AGB) and the predicted biomass value (mapped at 1-km grid cell resolution) and propagating these errors through the spatial modeling process (*SI Materials and Methods*). Errors in the distribution of forest aboveground biomass can be random or systematic in nature and can include the following: (*i*) *observation errors* associated with the uncertainty in estimates of Lorey's height from GLAS Lidar, errors associated with estimating AGB derived from GLAS Lidar height, and errors in estimating BGB from AGB (27); (*ii*) *sampling errors* associated with the spatial variability of AGB within a 1-km pixel and the representativeness and size of inventory plots and GLAS pixels over the landscape (29); and (*iii*) *prediction errors* associated with spatial analysis and mapping of AGB from significant contributions from satellite imagery (Fig. S3) (14, 30). We combined these three types of errors (*SI Materials and Methods*) to quantify the uncertainty of total biomass carbon stock as the 95% bootstrapped confidence interval at the 1-km pixel level (Fig. 3*B*). The overall uncertainty in mapping AGB at the pixel scale averaged over all continental regions is estimated at ±30%, but it is not uniform across regions or AGB ranges (±6% to ±53%) and depends on regional variations of forests, quality of remote sensing imagery, and sampling size and distribution of available ground and GLAS data. However, when averaged over all AGB ranges, regional uncertainties were comparable: ±27% over Latin America, ±32% over Africa, and ±33% over Asia (Fig. S4). The uncertainty in total carbon stock at the pixel scale averaged ±38% over all three continents after errors associated with BGB estimation were included in the analysis.

We computed the uncertainty around carbon estimates at national and regional scales by propagating errors associated with observation, including the errors associated with BGB estimates, sampling, and prediction. The uncertainty of carbon stock estimates at the national level was calculated as the square root of the sum of per-pixel errors for all pixels within the national boundary. This process reduced the relative errors as sample area increased. The national estimates were found to be constrained to within ±1% of the total carbon stock obtained

Table 1. Estimates of forest carbon stocks in the five largest national pools for each continent in the study region

	Canopy cover threshold								
	10%			25%			30%		
Country	Area (Mha)	Total C (Gt C)	C density (Mg C/ha)	Area (Mha)	Total C (Gt C)	C density (Mg C/ha)	Area (Mha)	Total C (Gt C)	C density (Mg C/ha)
Democratic Republic of Congo	205	24	118	177	23	128	164	22	134
Cameroon	36	5	129	30	4	142	27	4	151
Republic of Congo	28	4	144	24	4	160	23	4	162
Gabon	24	4	160	22	4	164	21	4	165
Angola*	73	3	44	42	3	66	34	2	70
Total sub-Saharan Africa	775	62	80	539	50	93	447	48	106
Brazil	596	61	102	481	56	116	442	54	123
Peru	80	12	153	75	12	158	73	12	160
Colombia	84	10	122	67	9	138	64	9	141
Venezuela	61	7	118	50	7	134	47	7	139
Bolivia	74	6	84	65	6	90	61	6	94
Total Latin America	1,209	120	99	977	110	112	893	107	119
Indonesia	165	23	142	127	20	155	121	19	158
Myanmar	49	7	146	42	6	155	40	6	157
Papua New Guinea	43	6	147	37	6	152	36	6	153
India†	63	6	89	43	4	104	36	4	112
Malaysia	30	5	172	25	5	179	25	4	180
Total Asia and Oceania	474	65	137	359	56	155	336	54	159
Total study region	2,458	246	100	1,875	215	115	1,677	208	124

All carbon values were calculated by using the pixel-based AGB value to compute BGB and total carbon (AGB + BGB). Carbon density (Mg C ha^{-1}) values were calculated from the ratio of total carbon to total forest area at national or regional levels.

*Central African Republic replaces Angola as no. 5 in Africa using 25% and 30% canopy cover thresholds.

†India switches from rank 4 to rank 5 using 25% and 30% canopy cover thresholds.

from averaging the pixel mean carbon values (Table S2). Spatial aggregation using different size windows shows that the error stays bounded to within ±5%, even at 10,000 ha (100 1-km pixels), due to the increased sample area. These errors do not include any systematic bias that may exist in biomass carbon allometry for AGB and BGB, in the in situ data inputs into the allometric equations (e.g., accurate botanical identifications for assigning wood density information, the wood density data itself, measurements of structure, etc.) or in the spatial sampling of forest biomass (*SI Materials and Methods*).

Discussion

The benchmark map provides a spatially refined and methodologically comparable carbon stock estimate for forests across 75 developing countries and improves upon previous assessments based on often old and incomplete national forest inventory data (27) and earlier spatial products (Fig. S5) (8, 14). Systematic quantification of the errors improves and constrains the pan-tropical estimate of total tropical forest biomass carbon (247 Gt C at 10% tree cover) and similarly national-scale carbon stocks (Table S3). Given the large uncertainty of forest carbon estimates for individual 1-km pixels (>30%), the map should be used primarily for national- and project-scale assessments (>10,000 ha). Reducing the uncertainty at the pixel level would require (*i*) higher-resolution data from future spaceborne radar and Lidar measurements to capture the spatial variability of forest structure and improve the estimation of aboveground biomass at spatial scales of <1 ha (21, 22) and (*ii*) in situ data with appropriate sampling schemes to match the scale of the remotely sensed measurements. Existing airborne Lidar and radar data can provide high-resolution estimates of project-scale forest carbon stocks (19, 21), but are likely to be unsuitable for large-scale wall-to-wall national- or continental-scale forest carbon monitoring systems.

Indeed, one key issue with any attempt to quantify forest carbon stocks is assessing the uncertainties inherent in estimating AGB from ground plots (29). Throughout this paper data associated with ground-based inventory plots have been assumed to be error-free. Although the methods used here do represent best estimates, estimating biomass from stem diameter, using continental or pan-tropical allometric equations, will introduce nonrandom errors, which may be significant and systematic (6, 29). Given the paucity of information on plot-based errors, we have

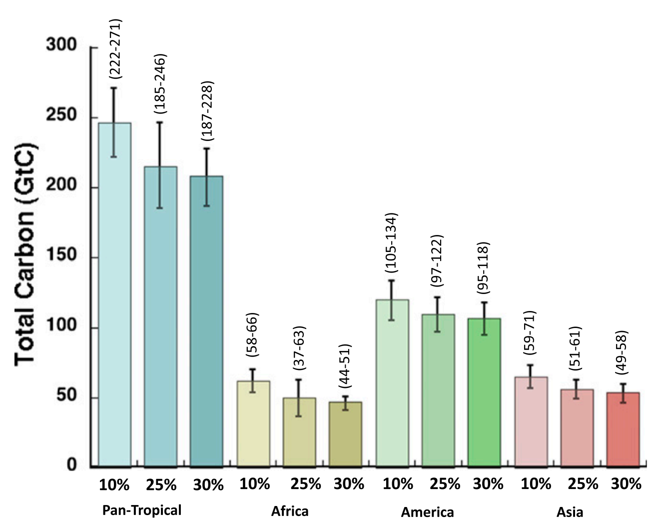

Fig. 4. Total carbon stock across the study region at three thresholds of canopy cover. Distribution of total (above- and belowground) biomass carbon stocks is shown. Carbon was computed by using the pixel-based AGB values to estimate root biomass and summing values across thresholds of percentage of tree cover (10%, 25%, and 30%) obtained from intersecting the 2001 MODIS vegetation continuous field (VCF) product (*SI Materials and Methods*) with the benchmark map. Similar distributions for each continent were produced separately. The error bars are based on the difference between the upper and lower limits of predicted AGB for computing total carbon (Table S2).

separated these from the other uncertainties considered in this study. By assuming that the systematic bias in estimating the carbon stock is approximately confined by the range of uncertainty of carbon predicted at the pixel level, we used the uncertainty bounds for each pixel to arrive at a range of estimates for total carbon (Fig. 4 and Table S3). However, these nonrandom errors associated with ground-based estimation of forest biomass will remain uncertain until consistent allometric equations within forest types or regions are developed.

All countries participating in a future policy mechanism to reduce emissions from deforestation and forest degradation will need to develop national- to regional-scale estimates of historic emissions (~2000–2010), which will be the starting point for generating reference emission levels. Most developing countries currently have limited data on carbon stocks of forests with which to estimate historic carbon emissions from past deforestation and degradation. Instead, countries often rely on estimates based on old or incomplete national forest inventories as reported by the Food and Agriculture Organization (31) or on Tier 1 biome-level estimates reported by the Intergovernmental Panel on Climate Change (32), neither of which are spatial in nature and thus do not allow for matching the carbon stock data with the areas undergoing change. The benchmark map presented here can assist country efforts by providing relatively fine-scale, spatially explicit and consistent forest carbon estimates that can be used with readily available remote sensing imagery to produce more robust estimates of historic emissions.

The benchmark map can also be used to assist countries in assessing the carbon emissions that are likely to be avoided by implementing different policies and programs aimed at reducing deforestation and forest degradation at regional and project scales. The map will assist developing country governments, land managers, policy makers, and civil society to become more informed about the likely result of their policies and programs in reducing national greenhouse gas emissions from the land-use sector.

Materials and Methods

Our methodological approach to mapping forest carbon stocks consists of four steps: (*i*) processing of ground and GLAS Lidar observations to sample forest structure and biomass over tropical regions, (*ii*) developing relations between Lidar-derived Lorey's height and AGB and between AGB and BGB, (*iii*) mapping AGB at 1-km spatial resolution using satellite imagery to stratify tropical forest types and structure and the Maximum Entropy (MaxEnt) approach to spatially model AGB, and (*iv*) assessing the uncertainty in modeling the spatial distribution of AGB by validating the results and propagating the errors through the methodology to estimate the total carbon stock and its uncertainty at the national scale.

Ground data used to train the biomass prediction model were derived from various sources including published literature and national forest inventories collected by the authors and their colleagues. The plots covered a variety of forest types on each continent, including old growth moist and wet tropical forest, woodland savanna, dry forest, peat swamp forest, and forests recovering from past disturbance or clearing. To compensate for the lack of systematic spatial sampling of aboveground biomass from ground measurements, we included >3 million AGB values calculated from Lidar measurements of forest vertical structure. We used 493 calibration plots distributed over forests across three continents to convert Lorey's height inferred from Lidar measurements to AGB and used tree allometry to estimate BGB from AGB. We estimated the total biomass per plot as the sum of AGB and BGB estimates and converted the results to carbon content by using a conversion factor of 0.5. To scale our plot- and Lidar-based AGB results over the landscape, we used nonparametric spatial modeling using the MaxEnt model, which included three steps: (*i*) compilation of the spatially gridded remote sensing data, (*ii*) implementation of MaxEnt and the production of the AGB map, and (*iii*) estimation of prediction uncertainty. We estimated the overall uncertainty in the final benchmark map by combining the errors associated with four independent terms: measurement errors, allometry errors, sampling errors, and prediction errors. Detailed information on each step is provided in *SI Materials and Methods*.

ACKNOWLEDGMENTS. We thank J. Reitsma, H. Woell, J. Woods, A. Daniels, S. Chinekan, and the Forest Developments Authority (Liberia) for assistance in processing inventory plots. This work was carried out under Contract 7150484 between Winrock International and The World Bank Group. The original remote sensing data were distributed online and were compiled and processed at the Jet Propulsion Laboratory, California Institute of Technology from previous National Aeronautics and Space Administration grants. The integrated remote sensing and distribution model was developed at the University of California, Los Angeles, Institute of Environment from previous National Aeronautics and Space Administration and National Science Foundation grants. The Blue Moon Fund supported forest inventory plots in the Peruvian Amazon for Lidar calibration.

1. Denman KL, et al. (2007) *IPCC Climate Change 2007: The Physical Science Basis*, eds Solomon S, et al. (Cambridge Univ Press), pp 499–587.
2. Schrope M (2009) When money grows on trees. *Nat Rep Climate Change* 3:101–103.
3. Van der Werf GR, et al. (2009) CO2 emissions from forest loss. *Nat Geosci* 2:737–738.
4. Dixon RK, et al. (1994) Carbon pools and flux of global forest ecosystems. *Science* 263:185–190.
5. Chave J, et al. (2008) Assessing evidence for a pervasive alteration in tropical tree communities. *PLoS Biol* 6:e45.
6. Lewis SL, et al. (2009) Increasing carbon storage in intact African tropical forests. *Nature* 457:1003–1006.
7. Field CB, Behrenfeld MJ, Randerson JT, Falkowski P (1998) Primary production of the biosphere: Integrating terrestrial and oceanic components. *Science* 281:237–240.
8. Gibbs HK, Brown S, Niles JO, Foley JA (2007) Monitoring and estimating tropical forest carbon stocks: Making REDD a reality. *Environ Res Lett* 2:045023.
9. Houghton RA (2005) Aboveground forest biomass and the global carbon balance. *Glob Change Biol* 11:945–958.
10. Ramankutty N, et al. (2007) Challenges to estimating carbon emissions from tropical deforestation. *Glob Change Biol* 13:51–66.
11. Hansen MC, et al. (2008) Humid tropical forest clearing from 2000 to 2005 quantified by using multitemporal and multiresolution remotely sensed data. *Proc Natl Acad Sci USA* 105:9439–9444.
12. Achard F, et al. (2002) Determination of deforestation rates of the world's humid tropical forests. *Science* 297:999–1002.
13. Houghton RA, Lawrence KT, Hackler JL, Brown S (2001) The spatial distribution of forest biomass in the Brazilian Amazon: A comparison of estimates. *Glob Change Biol* 7:731–746.
14. Saatchi SS, et al. (2007) Distribution of aboveground live biomass in the Amazon basin. *Glob Change Biol* 13:816–837.
15. Brown S, Gaston G (1996) *Tropical Africa: Land Use, Biomass, and Carbon Estimates for 1980 (CDIAC NDP-055, ORNL/CDIAC-92)*, CDIAC Communications, No. 23, Spring 1997 (Oak Ridge National Laboratory, Oak Ridge, TN), pp 12.
16. Cairns MA, Brown S, Helmer EH, Baumgardner GA (1997) Root biomass allocation in the world's upland forests. *Oecologia* 111:1–11.
17. Gibbs HK, Brown S (2000) Geographical distribution of woody biomass carbon stocks in tropical Africa: An updated database for 2000. Available at http://cdiac.ornl.gov/epubs/ndp/ndp0555/ndp05b.html from the Carbon Dioxide Information Center, Oak Ridge National Laboratory, Oak Ridge, TN. Accessed 2009.
18. Loarie SR, Asner GP, Field CB (2009) Boosted carbon emissions from Amazon deforestation. *Geophys Res Lett* 36:L14810.
19. Saatchi S, et al. (2011) Impact of spatial variability of tropical forest structure on Radar estimation of aboveground biomass. *Remote Sens Environ*, 10.1016/j.rse.2010.02.022.
20. Drake JB, et al. (2002) Estimation of tropical forest structural characteristics using large-footprint Lidar. *Remote Sens Environ* 79:305–319.
21. Asner GP, et al. (2010) High resolution forest carbon stock and emissions in the Amazon. *Proc Natl Acad Sci USA* 107:16738–16742.
22. Shugart HH, Saatchi S, Hall F (2010) A primer on the structure of forest and it measurements from space. *J Geophys Res Biogeosci* 115:G00E13.
23. Lefsky MA (2010) A global forest canopy height map from the Moderate Resolution Imaging Spectroradiometer and the Geoscience Laser Altimeter System. *Geophys Res Lett* 37:L15401.
24. Laurance WF (2007) Forest destruction in tropical Asia. *Curr Sci* 93:1544–1550.
25. Malhi Y, et al. (2006) The regional variation of aboveground live biomass in old-growth Amazonian forests. *Glob Change Biol* 12:1107–1138.
26. Slik JWF, et al. (2010) Environmental correlates of tree biomass, basal area, wood specific gravity, and stem density gradients in Borneo tropical forests. *Glob Ecol Biogeogr* 19:50–60.
27. Mokany K, Raison RJ, Prokushkin AS (2006) Critical analysis of root:shoot ratios in terrestrial biomes. *Glob Change Biol* 12:84–96.
28. Annex to UNFCCC decision 16/CMP.1. Available at http://unfccc.int/resource/docs/2005/cmp1/eng/08a03.pdf. Accessed 2010.
29. Chave J, et al. (2004) Error propagation and scaling for tropical forest biomass estimates. *Philos Trans R Soc Lond B Biol Sci* 359:409–420.
30. Köhl M, Baldauf T, Plugge D, Krug J (2009) Reduced emissions from deforestation and forest degradation (REDD): A climate change mitigation strategy on a critical track. *Carbon Balance Manag* 4:1–10.
31. Food and Agriculture Organization (2010) *Global Forest Resources Assessment 2010*, FAO Forestry Paper 163 (Food and Agriculture Organization, Rome).
32. Paustian K, Ravindranath NH, Van Amstel A (2006) (coordinating lead authors); Intergovernmental Panel on Climate Change (2006) *2006 IPCC Guidelines for National Greenhouse Gas Inventories,* Agriculture, Forestry and Other Land Use, Vol 4, Prepared by the National Greenhouse Gas Inventories Programme, [Institute for Global Environmental Strategies (IGES), Tokyo, Japan]. Available at http://www.ipcc-nggip.iges.or.jp/public/2006gl/vol1.htm. Accessed 2010.